Population extinction in a time-modulated environment

Michael Assaf,[1] Alex Kamenev,[2] and Baruch Meerson[1]
[1]*Racah Institute of Physics, Hebrew University of Jerusalem, Jerusalem 91904, Israel*
[2]*Department of Physics, University of Minnesota, Minneapolis, Minnesota 55455, USA*
(Received 30 July 2008; published 27 October 2008)

The extinction time of an isolated population can be exponentially reduced by a periodic modulation of its environment. We investigate this effect using, as an example, a stochastic branching-annihilation process with a time-dependent branching rate. The population extinction is treated in eikonal approximation, where it is described as an instanton trajectory of a proper reaction Hamiltonian. The modulation of the environment perturbs this trajectory and synchronizes it with the modulation phase. We calculate the corresponding change in the action along the instanton using perturbation techniques supported by numerical calculations. The techniques include a first-order theory with respect to the modulation amplitude, a second-order theory in the spirit of the Kapitsa pendulum effect, and adiabatic theory valid for low modulation frequencies.

DOI: 10.1103/PhysRevE.78.041123 PACS number(s): 05.40.−a, 87.23.Cc, 02.50.Ga

I. INTRODUCTION

Extinction of species after maintaining a long-lived quasistationary self-regulating population is a striking manifestation of large deviations coming from intrinsic stochasticity of processes of birth-death type. Not surprisingly, the extinction phenomenon is at the center stage of population biology and epidemiology [1]. More recently, it has attracted interest in the context of cell biochemistry [2]. As birth-death processes are usually far from equilibrium, they are also of much interest to physics [3,4]. Birth-death processes often occur in a time-varying environment, and the variations of the environment manifest themselves as an explicit time dependence of the birth and/or death rates. Elucidating different regimes of *exponential* reduction of the mean time to extinction (MTE) of species due to the time variation of the process rates is both important and interesting [5]. There is a large body of work on the effects of environmental *noise* on the MTE of birth-death systems. Early theoretical works on this subject assumed that the environmental noise which modulates the rates is delta correlated [6,7]. More recently, effects of finite correlation time of the noise have also been addressed in numerical simulations [8]. Not surprisingly, the simulation results provide only a partial understanding of the complex interplay between the nonlinear kinetics and intrinsic stochasticity of the self-regulating population on the one hand, and the magnitude and spectral and correlation properties of the environmental noise on the other hand. To get more insight into this type of problems, we will follow the recent work of Escudero and Rodríguez [9] and consider a much simpler model, where the time variation of the environment, as manifested in the rate modulation, is *periodic* in time. Although completely ignoring the noise aspect, this model enables one to investigate, in a controlled and often analytic way, different frequency and amplitude regimes of response of a self-regulating birth-death system to the rate modulations. Furthermore, not all environmental variations are noisy: some of them (such as daily, monthly, and annual cycles) occur in an almost periodic fashion.

The main objective of this work is to calculate, in different regimes of parameters, the exponential reduction in the MTE of birth-death systems due to a sinusoidal rate modulation. These calculations are intimately related to finding the "optimal path to extinction," or instanton connection in birth-death systems [10,11]. The instanton connection emerges in eikonal approximation to the original master equation, and it describes the most probable sequence of events that brings the birth-death system from its long-lived quasistationary state to extinction. As a prototypical example we will consider the stochastic branching-annihilation process $A\xrightarrow{\lambda}2A$ and $2A\xrightarrow{\mu}\varnothing$. This single-species birth-death process can be viewed as a simplified version of the well-known Verhulst logistic model [12]. Its constant-rate version was previously analyzed by a number of methods employing the large parameter $\Omega\equiv\lambda/\mu\gg 1$ that corresponds to a large average number of individuals in the quasistationary state at times short compared to the MTE [11,13–15].

The main theoretical tool that we employ in this work is an eikonal method which assumes that $\Omega\gg 1$. We apply the eikonal method to the exact evolution equation for the probability generating function that encodes the original continuous-time master equation [3,4]. In the leading order of the eikonal approximation, the evolution equation for the probability generating function reduces to a Hamilton-Jacobi equation, with an effective Hamiltonian that explicitly depends on time. We explore, analytically and numerically, the phase trajectories generated by this Hamiltonian and find the perturbed instanton: a perturbed heteroclinic phase trajectory that corresponds to extinction. Calculating the action along the instanton yields an approximation for the logarithm of the MTE [10,11]. Because of the explicit time dependence of the eikonal Hamiltonian, analytical progress is possible only via perturbation approaches. Therefore we use the eikonal method in conjunction with two different perturbation techniques that employ additional small parameters. The first of them is linear theory (LT): a theory based on linearization of Hamilton equations with respect to the modulation amplitude. For birth-death processes, the LT has been recently used by Escudero and Rodríguez [9]. A closely related theory was earlier developed by Dykman *et al.* [16,17] in the context of large fluctuations and escape in continuous (Langevin-type) stochastic systems driven by a time-periodic

signal. Dykman *et al.* showed that in LT the modulation signal removes the degeneracy of the unperturbed instanton trajectories with respect to time shift. This leads to the selection of the optimal instanton which is synchronized with the phase of the modulation signal. In general, the action along the optimal instanton is smaller than the action along the unperturbed instanton, leading to an exponential reduction of the escape time [16,17].

By employing a theorem due to Melnikov [18,19], Escudero and Rodríguez [9] proved the existence of a perturbed instanton in the branching-annihilation process with *weakly* modulated reaction rates. We extend the LT by calculating analytically the action along the instanton, which yields the logarithm of MTE. We also show numerically that the perturbed instanton persists for *any* reasonable modulation amplitudes, and for all modulation frequencies. Furthermore, we show that the LT gives satisfactory results only when the modulation frequency ω is smaller than or comparable with the relaxation rate of the system λ. When $\omega \gg \lambda$, the first-order correction to action, as predicted by the LT, turns out to be exponentially small with respect to the rescaled frequency ω/λ. It is the second-order correction in the modulation amplitude that becomes dominant in this regime. We calculate this correction by employing (a Hamiltonian extension of) the Kapitsa method, see, e.g., [20].

The opposite, low-frequency regime is both the simplest and most important as, for the same modulation amplitude, the exponential reduction of the MTE turns out to be the largest here. This regime can be efficiently dealt with in adiabatic approximation, for any reasonable modulation amplitude. Here one assumes that the extinction rate corresponding to the unperturbed problem is known, obtains the instantaneous extinction rate and averages it over the modulation period. This simple procedure yields the average extinction rate, and hence the MTE, of the perturbed problem. If the knowledge of the extinction rate of the unperturbed problem includes a pre-exponent, the adiabatic approximation yields a (modified) pre-exponent of the MTE of the perturbed problem: a significant improvement over the leading order of the eikonal method.

The remainder of the paper is organized as follows. We begin Sec. II with a brief introduction to the eikonal theory of extinction in birth-death processes with *time-independent* rates using the branching-annihilation model as an example. In Sec. III we present the eikonal theory of population extinction for a time-periodic rate modulation. We begin Sec. III by developing the LT, and continue by addressing the high-frequency limit $\omega \gg \lambda$ and employing the Kapitsa method. We conclude Sec. III by reporting numerical solutions of the Hamilton equations, in order to verify our theoretical results and extend them beyond the validity domain of the perturbation techniques. Section IV deals with the low-frequency limit by means of adiabatic approximation. Theoretical results obtained in this limit are compared with numerical solutions of the master equation. Section V presents a brief summary and discussion of our results.

II. MASTER EQUATION, PROBABILITY GENERATING FUNCTION, AND GEOMETRICAL OPTICS OF EXTINCTION

Here we present a brief introduction into an eikonal theory of population extinction in a time-independent environment [10,11], using the prototypical example of the branching-annihilation process $A \xrightarrow{\lambda} 2A$ and $2A \xrightarrow{\mu} \varnothing$, where λ, $\mu > 0$ are the reaction rate constants [11,13–15]. We assume in this section that λ and μ are independent of time.

At the level of deterministic modeling, the dynamics of the average number of individuals $\bar{n}(t)$ is described by the (mean-field) rate equation

$$\frac{d\bar{n}}{dt} = \lambda \bar{n} - \mu \bar{n}^2. \tag{1}$$

This equation predicts an attracting fixed point $\bar{n} = \lambda/\mu \equiv \Omega \gg 1$. The rate equation ignores the intrinsic noise that comes from the discreteness of individuals and stochastic character of the reactions. This noise determines the *probability distribution* of the actual values of n and, in particular, a quasistationary distribution around the average value $\Omega \gg 1$ that sets in on a relaxation time scale λ^{-1}; see below. On this time scale the mean-field picture correctly describes the average number of individuals in the stochastic process. At sufficiently long times, however, the noise invalidates the mean-field picture completely due to the existence, in the stochastic process, of the absorbing state $n=0$. In other words, the stochastic process $A \to 2A$ and $2A \to \varnothing$ eventually suffers a rare sequence of events that brings the system into the empty state.

The intrinsic noise is accounted for quantitatively by the master equation which describes the time evolution of $\mathcal{P}_n(t)$: the probability to have n individuals at time t. In the branching-annihilation example, the continuous-time master equation, for $n \geqslant 1$, reads

$$\frac{d\mathcal{P}_n(t)}{dt} = \frac{\mu}{2}[(n+2)(n+1)\mathcal{P}_{n+2}(t) - n(n-1)\mathcal{P}_n(t)] + \lambda[(n-1)\mathcal{P}_{n-1}(t) - n\mathcal{P}_n(t)]. \tag{2}$$

The master equation can be conveniently recast with the help of the probability generating function [3,4]

$$G(\wp,t) = \sum_{n=0}^{\infty} \wp^n \mathcal{P}_n(t), \tag{3}$$

where $\wp$ is an auxiliary variable. $G(\wp,t)$ encodes all the probabilities $\mathcal{P}_n(t)$, as the latter ones are given by the coefficients of the Taylor expansion of $G(\wp,t)$ around $\wp=0$. As the probabilities are normalizable to 1, $\Sigma_0^{\infty}\mathcal{P}_n(t)=1$, the generating function satisfies the condition

$$G(1,t) = 1. \tag{4}$$

The time-dependent moments of the distribution $\mathcal{P}_n(t)$ can be expressed through the derivatives of the generating function at $\wp=1$, e.g., $\langle n \rangle(t) \equiv \Sigma_n n\mathcal{P}_n(t) = \partial_{\wp} G(\wp,t)|_{\wp=1}$.

After a simple algebra, Eq. (2) can be transformed into an exact evolution equation for $G(\wp,t)$:

$$\frac{\partial G}{\partial t} = \frac{\mu}{2}(1-\wp^2)\frac{\partial^2 G}{\partial \wp^2} + \lambda\wp(\wp-1)\frac{\partial G}{\partial \wp}. \tag{5}$$

The absorbing state at $n=0$ corresponds to the stationary solution $G_s(\wp)=1$. The presence of the absorbing state is manifested by the absence in Eq. (5) of a term proportional to $G(\wp,t)$.

An initial value problem for Eq. (5) can be solved by expanding $G(\wp,t)$ in the eigenmodes of a Sturm-Liouville problem related to the non-Hermitian operator

$$\hat{\mathcal{H}} = \frac{\mu}{2}(1-\wp^2)\frac{\partial^2}{\partial \wp^2} + \lambda\wp(\wp-1)\frac{\partial}{\partial \wp};$$

see Ref. [15] for details. As in many other problems of extinction of species, there is a zero eigenvalue $E_0=0$ which describes the absorbing state, and an infinite discrete set of eigenvalues $\{E_n\}_{n=1}^{\infty}$ which describe an exponential decay with time of the rest of eigenmodes [15,21]. For $\Omega \gg 1$ the eigenvalue E_1 is exponentially small in Ω, and much less than the eigenvalues $E_2, E_3, \ldots$, which are of the order of the relaxation rate of the system λ. Therefore there are two widely different time scales in the problem. The decay, on the time scale λ^{-1}, of the higher eigenmodes corresponds to a rapid relaxation of the probability distribution $\mathcal{P}_n(t)$ to the quasistationary distribution, peaked at $n \simeq \Omega$. The much slower decay, on the time scale E_1^{-1}, of the lowest excited eigenmode [accompanied by a slow growth of the extinction probability $\mathcal{P}_0(t)$] corresponds to an exponentially slow decay of the quasistationary distribution and to extinction of the species. A simple approximation to the eigenvalue E_1 is provided by the leading order of the eikonal approximation [11]. Although it gives only exponential accuracy, it can be readily applied to systems of two species [22,23] and to time-dependent problems [9,23,24]: the focus of the present work.

Employing the eikonal ansatz $G(\wp,t)=\exp[-S(\wp,t)]$ in Eq. (5) and neglecting $\partial^2 S/\partial \wp^2$, we arrive at a Hamilton-Jacobi equation for $S(\wp,t)$ in the $\wp$ representation:

$$\frac{\partial S}{\partial t} + \frac{\mu}{2}(1-\wp^2)\left(\frac{\partial S}{\partial \wp}\right)^2 - \lambda\wp(\wp-1)\frac{\partial S}{\partial \wp} = 0. \tag{6}$$

Introducing a canonically conjugate coordinate $q=-\partial S/\partial \wp$ and shifting the momentum $p=\wp-1$, we arrive at a one-dimensional Hamiltonian flow, where p plays the role of the momentum [11]:

$$H(q,p) = \left[\lambda(1+p) - \frac{\mu}{2}(2+p)q\right]qp. \tag{7}$$

The Hamilton equations are

$$\dot{q} = \frac{\partial H}{\partial p} = q[\lambda(1+2p) - \mu(1+p)q], \tag{8}$$

$$\dot{p} = -\frac{\partial H}{\partial q} = p[\mu(2+p)q - \lambda(1+p)]. \tag{9}$$

As the eikonal Hamiltonian (7) does not depend explicitly on time, it is conserved: $H(q,p)=E=\text{const}$, and the problem is integrable. The phase plane (q,p), defined by this Hamiltonian flow, provides a useful visualization of the dynamics; see Fig. 1. The attracting fixed point $\bar{n}=\Omega$ and the repelling fixed point $\bar{n}=0$ of the one-dimensional rate equation (1) become hyperbolic points $A(q=\Omega,p=0)$ and $O(q=0,p=0)$ of the phase plane (q,p). They belong to the mean-field zero-energy line $p=0$. [The equality $H(q,0)=0$ reflects the probability conservation.] Another zero-energy line is the extinction line $q=0$. Of special importance, however, is the nontrivial zero-energy line

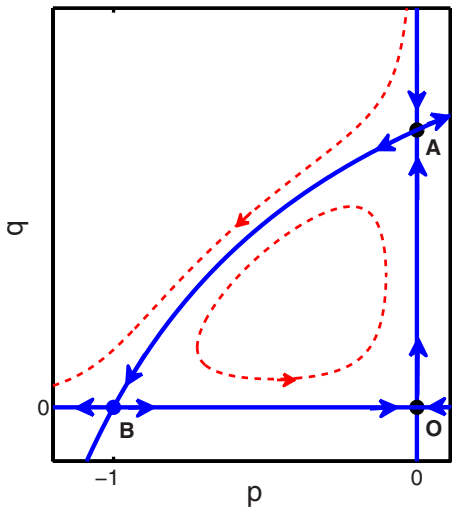

FIG. 1. (Color online) The phase plane of the unperturbed Hamiltonian (7). The solid lines denote zero-energy trajectories.

$$q = q_0(p) = \frac{2\Omega(1+p)}{(2+p)}. \tag{10}$$

This line, which includes still another hyperbolic fixed point $B(q=0,p=-1)$ (we call it the fluctuational point), gives a leading-order description of the quasistationary probability distribution. The $-1 \leqslant p \leqslant 0$ segment of this line is a heteroclinic trajectory. It exits, at time $t=-\infty$, the hyperbolic fixed point A along its unstable manifold and enters, at time $t=\infty$, the hyperbolic fixed point B along its stable manifold. The heteroclinic trajectory (often referred to as the optimal path to extinction, or the instanton [25–27]) describes the most probable sequence of events bringing the system from the quasistationary state to extinction. Up to a pre-exponent, that is missed by the leading order of the eikonal theory, the MTE can be approximated as $\tau_{ex} \sim \exp(\mathcal{S}_0)$, where

$$\mathcal{S}_0 = -\int_0^{-1} q_0(p)dp = 2\Omega(1-\ln 2). \tag{11}$$

The time-dependent instanton coordinate $q_0(t-t_0)$ and momentum $p_0(t-t_0)$ are the following:

$$q_0(t-t_0) = \frac{2\Omega}{2+e^{\lambda(t-t_0)}}, \quad p_0(t-t_0) = -\frac{1}{1+e^{-\lambda(t-t_0)}}, \tag{12}$$

where t_0 is an arbitrary time shift.

The eikonal approximation is valid when $\mathcal{S}_0 \gg 1$, that is $\Omega \gg 1$. Equation (11), obtained by Elgart and Kamenev [11], coincides with the leading order term of the logarithm of the MTE found by other methods (also employing the strong inequality $\Omega \gg 1$) by Turner and Malek-Mansour [13], Kessler and Shnerb [14], and Assaf and Meerson [15].

III. EXTINCTION IN A TIME-VARYING ENVIRONMENT: PERTURBATION TECHNIQUES FOR THE INSTANTON

Now let the branching rate λ in the master equation (2), and in the evolution equation (5) for $G(\wp,t)$, vary sinusoidally in time:

$$\lambda(t) = \lambda_0(1 + \varepsilon \cos \omega t), \tag{13}$$

where $|\varepsilon| < 1$, and ε and ω are the modulation amplitude and frequency, respectively. The eikonal approximation now yields the following *time-dependent* Hamiltonian:

$$H(q,p,t) = H_0(q,p) + \varepsilon H_1(q,p,t), \tag{14}$$

where

$$H_0(q,p) = \lambda_0(1+p)pq - \frac{\mu_0}{2}(2+p)pq^2, \tag{15}$$

and

$$H_1(q,p,t) = \lambda_0(1+p)pq \cos \omega t. \tag{16}$$

For the unperturbed Hamiltonian $H_0(q,p)$, the instanton (10) and the corresponding action $\mathcal{S}_0$ along it, Eq. (11), are known. Our strategy will be to calculate the action along the *perturbed* instanton: the instanton of the perturbed, time-dependent Hamiltonian (14).

Following Escudero and Rodríguez [9], let us consider the Poincaré map $P_\varepsilon^{t_0} = \{q,p,t | t = t_0 \in [0,T]\}$: the projection of three-dimensional trajectories of the nonautonomous system (14) in the (q,p,t) space on the (q,p) plane at section time $t_0 \in [0, 2\pi/\omega]$. In the perturbed system the hyperbolic points A and B are also perturbed. We will denote the perturbed fixed points by $A_\varepsilon^{t_0}$ and $B_\varepsilon^{t_0}$, respectively. For generic Hamiltonians the existence of the perturbed hyperbolic points is guaranteed, by the Poincaré-Birkhoff fixed point theorem [19], only for sufficiently small ε. For the birth-death Hamiltonian we are dealing with here the perturbed fixed points exist for *any* $|\varepsilon| < 1$. The point $B_\varepsilon^{t_0} = (q=0, p=-1)$ remains unchanged [28], whereas the point $A_\varepsilon^{t_0}$ can be easily found from the time-dependent rate equation (8) with $p=0$ and λ from Eq. (13):

$$\dot{q} = q[\lambda_0(1 + \varepsilon \cos \omega t) - \mu q]. \tag{17}$$

The solution of this equation, for an arbitrary initial condition $q(0)$, is the following:

$$q(t) = \frac{q(0)\exp\{\lambda_0 t + [\varepsilon\lambda_0 \sin(\omega t)/\omega]\}}{1 + \frac{\mu_0}{\lambda_0} q(0) \int_0^{\lambda_0 t} \exp\{s + [\varepsilon\lambda_0 \sin(\omega s/\lambda_0)/\omega]\} ds}, \tag{18}$$

see also Ref. [9]. At long times this solution becomes periodic in time, and can be written as

$$q(t) = \frac{\lambda_0}{\mu_0} \frac{\exp[\varepsilon\lambda_0 \sin(\omega t)/\omega]}{\sum_{n=-\infty}^{\infty} I_n(\varepsilon\lambda_0/\omega)\cos(n\omega t - \phi_n - n\pi/2)/\sqrt{1 + n^2\omega^2/\lambda_0^2}}, \tag{19}$$

where $I_n(x)$ is the modified Bessel function, and $\phi_n = \arctan(n\omega/\lambda_0)$. Putting in Eq. (19) $t=t_0$ we obtain q of the perturbed fixed point $A_\varepsilon^{t_0}$, whereas its p remains zero.

Existence of the perturbed fixed points is a necessary but, in general, insufficient condition for the existence of a heteroclinic trajectory connecting the unstable manifold of $A_\varepsilon^{t_0}$ and the stable manifold of $B_\varepsilon^{t_0}$. In general, one should also establish the existence, in the perturbed problem, of the unstable and stable manifolds themselves, and of their intersection [9,19]. We verified analytically and numerically, see below, that the unstable manifold of $A_\varepsilon^{t_0}$ and the stable manifold of $B_\varepsilon^{t_0}$ do intersect. Let us denote the perturbed instanton connection by the pair $q(t,t_0), p(t,t_0)$. As the energy is not conserved, the action along the perturbed instanton now includes an integral of H over time:

$$\mathcal{S} = \int_{-\infty}^{\infty} \{p(t,t_0)\dot{q}(t,t_0) - H_0[q(t,t_0),p(t,t_0)] - \varepsilon H_1[q(t,t_0),p(t,t_0),t]\} dt, \tag{20}$$

where $\dot{q}(t,t_0) = dq/dt$, and the unperturbed Hamiltonian $H_0(q,p)$ is invariant to the specific choice of t_0. Escudero and Rodríguez [9] applied the Melnikov theorem [18,19] and proved that a perturbed instanton exists in this problem for sufficiently small ε. To this end they calculated (an approximation for) the distance between the unstable and stable manifolds, which is given by the Melnikov function, see below, and showed that it vanishes for a specific choice of t_0. We briefly reproduce their derivation in Sec. III A, along with additional results: a linear-theory calculation of the action (20) and the corresponding reduction in the logarithm of the MTE. We also show, in Sec. III B, that the perturbed instanton exists for high-frequency perturbations, $\omega \gg \lambda_0$ at any $|\varepsilon| < 1$. Furthermore, we report, in Sec. III C, strong numerical evidence that the perturbed instanton exists for any $|\varepsilon| < 1$ and any ω.

A. Linear correction to action

Here we consider the linear theory (LT) which assumes that the term $\varepsilon H_1(q,p,t)$ in Eq. (14) can be treated perturbatively. For this assumption to hold it is sufficient to demand the strong inequality $|\varepsilon| \ll 1$. As we will see in Sec. III B, at high frequencies, $\omega \gg \lambda_0$, the strong inequality $|\varepsilon| \ll 1$ becomes unnecessary. For completeness, we will derive Eqs.

(24) and (25) in a general form, before dealing with the particular example of branching and annihilation. In the first order in ε the perturbed instanton of $H(q,p,t)$ is described by the equations

$$q(t,t_0) = q_0(t-t_0) + \varepsilon q_1(t,t_0),$$

$$p(t,t_0) = p_0(t-t_0) + \varepsilon p_1(t,t_0), \tag{21}$$

where $q_0(t-t_0)$ and $p_0(t-t_0)$ stand for the (known) instanton solution of the unperturbed equations,

$$\dot{q}_0 = \frac{\partial H_0(q_0,p_0)}{\partial p_0},$$

$$\dot{p}_0 = -\frac{\partial H_0(q_0,p_0)}{\partial q_0}, \tag{22}$$

that is Eqs. (8) and (9) with $\lambda=\lambda_0$.

To calculate the action (20) we expand the integrand in ε and obtain, in the first order,

$$\begin{aligned}(p_0+\varepsilon p_1)(\dot{q}_0+\varepsilon\dot{q}_1) - H_0(q_0,p_0) - \varepsilon q_1\frac{\partial H_0(q_0,p_0)}{\partial q_0} \\ - \varepsilon p_1\frac{\partial H_0(q_0,p_0)}{\partial p_0} - \varepsilon H_1(q_0,p_0,t) \\ \simeq p_0\dot{q}_0 - H_0(q_0,p_0) + \varepsilon p_1\dot{q}_0 + \varepsilon p_0\dot{q}_1 + \varepsilon q_1\dot{p}_0 - \varepsilon p_1\dot{q}_0 \\ - \varepsilon H_1(q_0,p_0,t).\end{aligned} \tag{23}$$

After the integration the first two terms yield the unperturbed action $\mathcal{S}_0$. The third term cancels out with the sixth term, while the fourth term cancels out, after integration by parts, with the fifth term. The result is $\mathcal{S}(t_0)=\mathcal{S}_0+\Delta\mathcal{S}(t_0)$, where

$$\Delta\mathcal{S}(t_0) = -\varepsilon\int_{-\infty}^{\infty} H_1[q_0(t-t_0),p_0(t-t_0),t]dt. \tag{24}$$

Recall that the integration is performed along the unperturbed instanton. To find the *optimal* correction to action we have to *minimize* $\mathcal{S}(t_0)$ with respect to t_0 (compare to Refs. [16,17]). This yields the following equation for t_0:

$$\begin{aligned}\frac{d\mathcal{S}(t_0)}{dt_0} &= \varepsilon\int_{-\infty}^{\infty}\left(\frac{\partial H_1}{\partial q_0}\dot{q}_0 + \frac{\partial H_1}{\partial p_0}\dot{p}_0\right)dt \\ &\equiv -\varepsilon\int_{-\infty}^{\infty}\{H_0,H_1\}_0 dt = 0,\end{aligned} \tag{25}$$

where $\{H_0,H_1\}_0$ is the Poisson bracket evaluated on the unperturbed instanton. The quantity $M(t_0)=\int_{-\infty}^{\infty}\{H_0,H_1\}_0 dt$ is the Melnikov function of the perturbed problem [9,18,19]. It is proportional to the distance between the unstable and stable manifolds of $A_\varepsilon^{t_0}$ and $B_\varepsilon^{t_0}$, respectively [19]. That $M(t_0)$ has simple zeros yields a sufficient condition for the existence of the perturbed instanton. These zeros are the critical points of the function $\mathcal{S}(t_0)$. By finding the critical value of t_0 for which $\mathcal{S}(t_0)$ has its minimum, we obtain the minimal action along the instanton of the perturbed problem (24). It is the min $\Delta\mathcal{S}(t_0)$ that yields the reduction of the logarithm of the MTE, caused by the time dependence of the rate. Note that when H_0 commutes with H_1, $M(t_0)$ vanishes identically at any t_0, but this degenerate case is hardly of interest.

The validity of the linear eikonal theory is determined by the double strong inequality

$$1 \ll \Delta\mathcal{S} \ll \mathcal{S}_0. \tag{26}$$

The left inequality is required for the eikonal approximation to be valid, while the right inequality is needed for the linearization to be valid. Note that the rate variation does not have to be time periodic for the LT to hold: it suffices to demand that the rate variation be bounded by a sufficiently small value.

Now we return to the branching-annihilation example. In the first order in ε, the perturbed fixed point $A_\varepsilon^{t_0}$ is determined by the equation

$$\frac{q_A}{\Omega} = 1 + \frac{\varepsilon\lambda_0(\lambda_0\cos\omega t + \omega\sin\omega t)}{\omega^2+\lambda_0^2} \tag{27}$$

evaluated at $t=t_0$. Substituting Eqs. (12) and (16) in Eq. (24), we obtain

$$\Delta\mathcal{S}(t_0) = 2\varepsilon\Omega\int_{-\infty}^{\infty}\frac{\cos(\pi/\lambda_0+t_0)e^{\tau}}{(1+e^{\tau})^2(2+e^{\tau})}d\tau. \tag{28}$$

Calculating the integral we arrive at

$$\begin{aligned}\frac{\mathcal{S}(t_0)}{\mathcal{S}_0} = 1 + \frac{\pi\varepsilon}{(1-\ln 2)\sinh(\pi\omega/\lambda_0)} \\ \times\left\{\frac{\omega}{\lambda_0}\cos\omega t_0 - \sin\left[\omega\left(\frac{\ln 2}{\lambda_0}+t_0\right)\right] + \sin\omega t_0\right\},\end{aligned} \tag{29}$$

where $\mathcal{S}_0$ is given by Eq. (11). The minimal action is $\mathcal{S}(t_0^*)$, where t_0^* is the solution of the trigonometric equation for t_0:

$$\begin{aligned}\frac{d\mathcal{S}(t_0)}{dt_0} &\equiv -\varepsilon M(t_0) \\ &= -\frac{2\pi\varepsilon\Omega\omega}{\sinh(\pi\omega/\lambda_0)} \\ &\quad\times\left\{\frac{\omega}{\lambda_0}\sin\omega t_0 + \cos\left[\omega\left(\frac{\ln 2}{\lambda_0}+t_0\right)\right] - \cos\omega t_0\right\} \\ &= 0,\end{aligned} \tag{30}$$

subject to the condition $d^2\mathcal{S}(t_0)/dt_0^2>0$. The solution is

$$\omega t_0^* = \pi + \arctan\left[\frac{1-\cos(\alpha\ln 2)}{\alpha-\sin(\alpha\ln 2)}\right], \tag{31}$$

where $\alpha=\omega/\lambda_0$, and we assume here and in the remainder of this subsection that $\varepsilon>0$ [30]. Equation (31) shows that the optimal instanton becomes synchronized with the rate modulation, similarly to what happens in the context of escape in Langevin-type stochastic systems driven by a time-periodic signal [16,17]. Figure 2 depicts the difference $\omega t_0-\pi$ as a function of α. This difference is small at $\alpha\ll 1$, $\omega t_0-\pi \simeq (\ln 2)^2/[2(1-\ln 2)]\alpha$, and at $\alpha\gg 1$: $\omega t_0-\pi\simeq\alpha^{-1}[1-\cos(\alpha\ln 2)]$. It vanishes for $\alpha=2\pi n/\ln 2$, where n

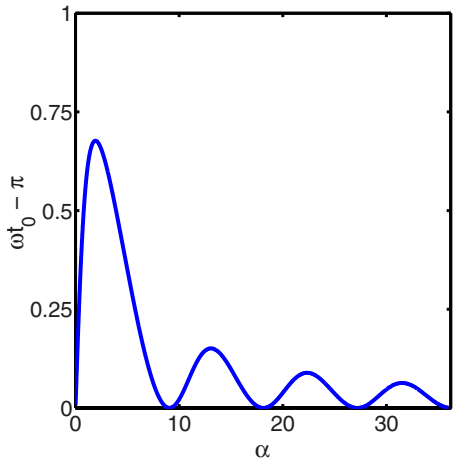

FIG. 2. (Color online) The difference $\omega t_0 - \pi$, see Eq. (31), as a function of $\alpha = \omega/\lambda_0$.

$=1,2,\ldots$. For $\alpha \sim 1$ the difference $\omega t_0 - \pi$ is of the order of one.

Now we use Eqs. (29) and (31) to find the perturbed action:

$$\frac{\mathcal{S}_{\min}}{\mathcal{S}_0} = 1 + \frac{\Delta\mathcal{S}}{\mathcal{S}_0} = 1 - \frac{\pi\varepsilon}{(1-\ln 2)\sinh(\pi\alpha)} \times \{[\sin(\alpha \ln 2) - \alpha]^2 + [\cos(\alpha \ln 2) - 1]^2\}^{1/2}. \quad (32)$$

Figure 3 depicts $\Delta\mathcal{S}/(\varepsilon\Omega)$ as a function of α as predicted by Eq. (32). The maximum effect of the rate modulation is obtained at $\alpha \to 0$. Recall that the perturbed action yields (in the leading order in Ω) the natural logarithm of the MTE of the perturbed branching-annihilation problem.

The perturbative eikonal result is valid as long as the double inequality (26) is obeyed. The left inequality breaks down at very small ε, whereas the right inequality breaks down at not small ε where linearization becomes invalid. One can define, in analogy with the problem of activated escape in Langevin-type stochastic systems [16], the logarithmic susceptibility $\chi = \partial(\Delta\mathcal{S})/\partial|\varepsilon|$. Within the framework of the LT [that is, for intermediate values of the modulation amplitude that satisfy the double inequality (26)], χ is independent of ε:

$$\chi = -\frac{2\pi\Omega}{\sinh(\pi\alpha)}\{[\sin(\alpha \ln 2) - \alpha]^2 + [\cos(\alpha \ln 2) - 1]^2\}^{1/2}. \quad (33)$$

At small and large modulation amplitudes χ becomes amplitude-dependent.

In the low-frequency limit, $\alpha \ll 1$, one obtains from Eq. (32)

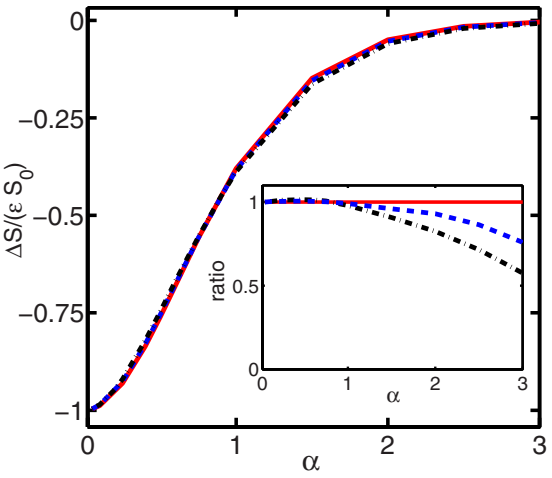

FIG. 3. (Color online) The correction to action $\Delta\mathcal{S}$, rescaled by $\varepsilon\mathcal{S}_0$, vs the rescaled modulation frequency $\alpha = \omega/\lambda_0$. Dashed and dash-dotted lines: predictions of the linear theory, $\Delta\mathcal{S}_{LT}$, see Eq. (32), for $\varepsilon = 0.04$ and $\varepsilon = 0.1$, respectively. Solid line: $\Delta\mathcal{S}_{num}$ found by solving the Hamilton equations numerically; see Sec. III C. On this scale the three lines are indistinguishable. The inset shows the ratios of $\Delta\mathcal{S}_{LT}$ and $\Delta\mathcal{S}_{num}$ for $\varepsilon = 0.04$ (the dashed line), and $\varepsilon = 0.1$ (the dash-dotted line). The disagreement at high frequencies demands an account of what we call the Kapitsa correction, calculated in Sec. III B.

$$\frac{\Delta\mathcal{S}}{\varepsilon\mathcal{S}_0} = -1 + \frac{\alpha^2}{6}\left[\pi^2 - \frac{(\ln 2)^3}{(1-\ln 2)^2} + \frac{(\ln 2)^4}{4(1-\ln 2)^2}\right], \quad (34)$$

where we have kept the leading and subleading terms. The leading term coincides with the prediction (63) from the adiabatic approximation; see Sec. IV. In this limit the LT is valid for $\Omega^{-1} \ll \varepsilon \ll 1$. The same criterion applies for $\alpha \sim 1$, as $\Delta\mathcal{S}/(\varepsilon\Omega)$ in Eq. (32) is of order 1 there. In the high-frequency limit, $\alpha \gg 1$, the correction $\Delta\mathcal{S}$ is exponentially small:

$$\frac{\Delta\mathcal{S}}{\varepsilon\mathcal{S}_0} = -\frac{2\pi\alpha e^{-\pi\alpha}}{1-\ln 2}. \quad (35)$$

Here ε need not be small compared to 1 to satisfy the right inequality in Eq. (26). Note that Eqs. (32)–(35) with ε replaced by $|\varepsilon|$ are valid also for $\varepsilon < 0$.

In Fig. 3 Eq. (32) is compared with the correction to action found by solving the Hamilton equations numerically (see Sec. III C for details of the numerics). One can see a good agreement at small and intermediate frequencies, and a disagreement at high frequencies. What is the reason for the disagreement? That the correction to action $\Delta\mathcal{S}$, as predicted by the LT, becomes exponentially small at large frequencies indicates that the ε^2 correction, neglected by the LT, becomes dominant there. This conjecture is validated in the next subsection, where we consider the high-frequency case and calculate the ε^2 correction using (a Hamiltonian extension of) the Kapitsa method.

B. Quadratic correction to action: The Kapitsa correction

Here we consider the high-frequency limit, $\omega \gg \lambda_0$ and calculate the correction to action which is of the second order in ε. To this end we use (a Hamiltonian extension of) the method that was developed long ago in the context of the "Kapitsa pendulum:" a rigid pendulum with a rapidly vibrating pivot, see, e.g., [20]. The Kapitsa method involves, as a first step, calculation of small high-frequency corrections to the unperturbed coordinate and momentum of the system. Because of the high frequency of the perturbation these corrections are small even if ε is of order 1. Using the high-frequency corrections, we construct a canonical transformation which, by means of time averaging (that is, by rectifying the high-frequency component of the motion), transforms the original time-dependent Hamiltonian into an effective *time-independent* one. The effective Hamiltonian includes a correction coming from the rectified high-frequency perturbation. Finally, we find the perturbed instanton, emerging from this effective time-independent Hamiltonian, and the action along the instanton.

The starting point of the derivation is the same Hamiltonian (14) with rates given by Eq. (13). We represent q and p as follows:

$$q(t) = X(t) + \xi(t), \quad p(t) = Y(t) + \eta(t), \tag{36}$$

where X and Y are slow variables, while ξ and η are small and rapidly oscillating. Now we expand the Hamiltonian $H(q,p,t)$ around $q=X$ and $p=Y$ up to the second order in ξ and η:

$$\begin{aligned} H(q,p,t) &\simeq H(X,Y,t) + \xi\frac{\partial H(X,Y)}{\partial X} + \eta\frac{\partial H(X,Y)}{\partial Y} \\ &+ \frac{\xi^2}{2}\frac{\partial^2 H(X,Y)}{\partial X^2} + \frac{\eta^2}{2}\frac{\partial^2 H(X,Y)}{\partial Y^2} + \xi\eta\frac{\partial^2 H(X,Y)}{\partial X \partial Y} \\ &\equiv \tilde{H}(X,Y,t). \end{aligned} \tag{37}$$

The Hamilton equations become

$$\dot{q} = \dot{X} + \dot{\xi} \simeq \frac{\partial \tilde{H}(X,Y,t)}{\partial Y}, \quad \dot{p} = \dot{Y} + \dot{\eta} \simeq -\frac{\partial \tilde{H}(X,Y,t)}{\partial X}. \tag{38}$$

Now we demand that the rapidly oscillating terms in Eqs. (38) balance each other. This yields

$$\dot{\xi} \simeq \varepsilon\lambda_0 X(2Y+1)\cos\omega t, \quad \dot{\eta} \simeq -\varepsilon\lambda_0 Y(Y+1)\cos\omega t, \tag{39}$$

where terms of the order of ξ and η have been neglected, but their time derivatives (which are proportional to ω and therefore large) have been kept. Treating X and Y as constants during the period of rapid oscillations $2\pi/\omega$, we can easily solve Eqs. (39) and obtain

$$\xi(t) \simeq \frac{\varepsilon\lambda_0}{\omega} X(2Y+1)\sin\omega t, \quad \eta(t) \simeq -\frac{\varepsilon\lambda_0}{\omega} Y(Y+1)\sin\omega t. \tag{40}$$

Now it is clear that this perturbation scheme demands $|\varepsilon|\lambda_0/\omega \ll 1$. As we have assumed $\omega \gg \lambda_0$, ε need not be small.

Using Eqs. (36) and (40), we perform an almost canonical transformation from the old variables q and p to the new variables X and Y:

$$\begin{aligned} q(X,Y,t) &= \frac{X}{1-(\varepsilon\lambda_0/\omega)(2Y+1)\sin\omega t} \\ &\simeq X\left[1 + \frac{\varepsilon\lambda_0}{\omega}(2Y+1)\sin\omega t + \frac{\varepsilon^2\lambda_0^2}{\omega^2}(2Y+1)^2\sin^2\omega t\right], \\ p(X,Y,t) &= Y\left[1 - \frac{\varepsilon\lambda_0}{\omega}(1+Y)\sin\omega t\right]. \end{aligned} \tag{41}$$

This transformation is canonical up to third order of $\mathcal{O}[(\lambda_0/\omega)^3] \ll 1$, as the Poisson brackets $\{q,p\}_{(X,Y)} = 1 + \mathcal{O}[(\lambda_0/\omega)^3]$. The generating function of this transformation is

$$F_2(q,Y,t) = qY[1-(\varepsilon\lambda_0/\omega)(Y+1)\sin\omega t],$$

see, e.g., Ref. [20]. Now we transform to the new variables X and Y, $H' = H + \partial F_2/\partial t$, and average the new Hamiltonian H' over the period of rapid oscillations $2\pi/\omega$. This yields an effective Hamiltonian

$$\begin{aligned} \bar{H}(X,Y) &= \lambda_0 XY(1+Y) - \frac{\mu_0}{2}(Y+2)YX^2 \\ &+ \frac{\varepsilon^2\lambda_0^2}{2\omega^2}XY\left[\lambda_0 Y(1+Y)^2 - \frac{\mu_0}{2}(2+12Y+18Y^2+5Y^3)\right] \end{aligned} \tag{42}$$

which is time-independent. The first two terms come from the unperturbed Hamiltonian, Eq. (15), the other two terms describe a rectified ε^2 correction coming from the high-frequency perturbation. The mean-field fixed point and fluctuational fixed point of the effective Hamiltonian are

$$A\left[q = \Omega\left(1 - \frac{\lambda^2\varepsilon^2}{2\omega^2}\right), p = 0\right] \quad \text{and} \quad B(q=0, p=-1),$$

respectively. As the effective Hamiltonian is time-independent, there is no need for the Poincaré section in this limit. Two "trivial" zero-energy lines of the effective Hamiltonian are $X=0$ and $Y=0$. The nontrivial zero-energy line yields the effective instanton $X_0(Y)$. In the leading order of $\alpha \equiv \omega/\lambda_0 \gg 1$ we obtain

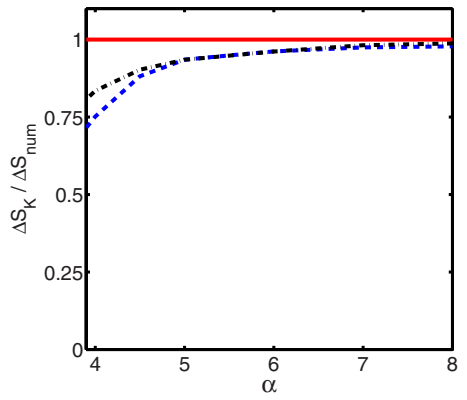

FIG. 4. (Color online) The ratio of the Kapitsa correction $\Delta\mathcal{S}_K$, Eq. (46), and $\Delta\mathcal{S}_{num}=\mathcal{S}_{num}-2\Omega(1-\ln 2)$ for $\varepsilon=0.1$ (dashed line) and $\varepsilon=0.2$ (dash-dotted line), vs $\alpha=\omega/\lambda_0$. The agreement improves with an increase of α and ε.

$$X_0(Y) \simeq \frac{2\Omega(1+Y)}{2+Y}\left[1-\frac{\varepsilon^2(2+10Y+15Y^2+4Y^3)}{2\alpha^2(2+Y)}\right]. \tag{43}$$

The action along the effective instanton is

$$\mathcal{S}=-\int_0^{-1} X_0(Y)dY=\mathcal{S}_0\left(1-\frac{K\varepsilon^2}{\alpha^2}\right), \tag{44}$$

where

$$K=\frac{6\ln 2-49/12}{1-\ln 2}=0.2462\ldots. \tag{45}$$

We will call the resulting correction to the unperturbed action,

$$\Delta\mathcal{S}_K=-K\mathcal{S}_0(\varepsilon/\alpha)^2, \tag{46}$$

the Kapitsa correction. The eikonal approximation, that has led to Eq. (46), demands $\Delta\mathcal{S}_K\gg 1$. Figure 4 shows the ratio of $\Delta\mathcal{S}_K$ and the correction to action, found by solving the Hamilton equations numerically (see Sec. III C for details of the numerics). As expected, good agreement is observed at high frequencies, where the Kapitsa method is applicable.

Now we can put the results obtained with the LT and with the Kapitsa method into a broader context. The correction to the unperturbed action $\Delta\mathcal{S}=\mathcal{S}-\mathcal{S}_0<0$ must have the following general form:

$$\frac{\Delta\mathcal{S}}{\mathcal{S}_0}=-f_1(\alpha)|\varepsilon|-f_2(\alpha)\varepsilon^2+\cdots. \tag{47}$$

(Clearly, $\Delta\mathcal{S}$ must be analytical in $|\varepsilon|$, rather than in ε, as changing the sign of ε only brings about a phase shift π which changes the minimum point t_0 but leaves the minimum action unchanged.) The function $f_1(\alpha)>0$ is given by the LT, see Eq. (32):

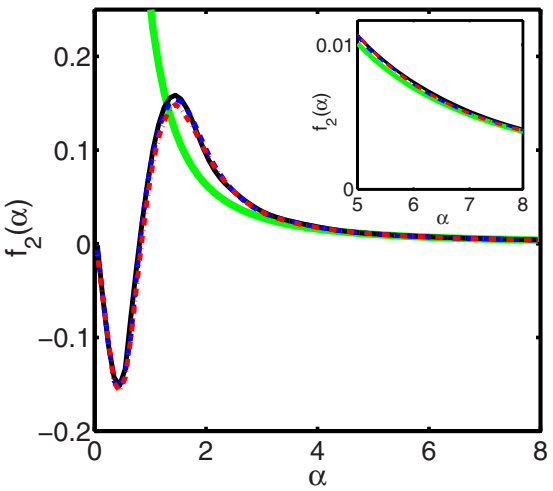

FIG. 5. (Color online) Shown is the function $f_2(\alpha)$ determined numerically; see text. The curves for $\varepsilon=0.04$ (solid line), $\varepsilon=0.1$ (dashed line), and $\varepsilon=0.2$ (dash-dotted line) collapse into a single curve as expected from Eq. (47). The $\alpha\gg 1$ asymptote of $f_2(\alpha)$, given by Eq. (49) (thick solid line), agrees with the numerical result at high frequencies. The inset shows a blowup of the high-frequency region.

$$f_1(\alpha)=\frac{\pi\{[\sin(\alpha\ln 2)-\alpha]^2+[\cos(\alpha\ln 2)-1]^2\}^{1/2}}{(1-\ln 2)\sinh(\pi\alpha)}. \tag{48}$$

The high-frequency asymptote of $f_2(\alpha)$ is given by Eq. (44):

$$f_2(\alpha)=\frac{K}{\alpha^2},\quad \alpha\gg 1. \tag{49}$$

To calculate the function $f_2(\alpha)$ analytically for all α would be quite cumbersome, so we found it numerically by solving the Hamilton equations for three different values of ε and for different frequencies (see Sec. III C for details of the numerics). For each set of ε and α we computed $\Delta\mathcal{S}$ and used Eq. (47) with $f_1(\alpha)$ from Eq. (48) to extract $f_2(\alpha)$. As expected, the resulting plots of $f_2(\alpha)$ for different ε collapse into a single curve; see Fig. 5. Noticeable is a nonmonotonic, alternating-sign α dependence. The high-frequency asymptote of $f_2(\alpha)$ is in excellent agreement with the Kapitsa correction (49). Note that $f_2(\alpha)$ vanishes as $\alpha\to 0$. The reason is that, as $\omega\to 0$, the dependence of the eikonal part of $\Delta\mathcal{S}$ on ε becomes linear; see Sec. IV. This is a nongeneric property of the case when the branching rate λ is modulated, while the annihilation rate μ is not.

When does the Kapitsa correction to action dominate over the exponentially small first-order correction at high frequencies? The corresponding condition $\varepsilon^2 f_2(\alpha)\gg|\varepsilon|f_1(\alpha)$ can be rewritten as $|\varepsilon|\gg\alpha^3 e^{-\pi\alpha}$; it is easily satisfied for large α. In this regime the logarithmic susceptibility χ is proportional to $|\varepsilon|$.

C. Numerical calculations of the perturbed instanton and the action

To verify our analytical results, and to explore the parameter regions beyond the validity of the perturbation methods,

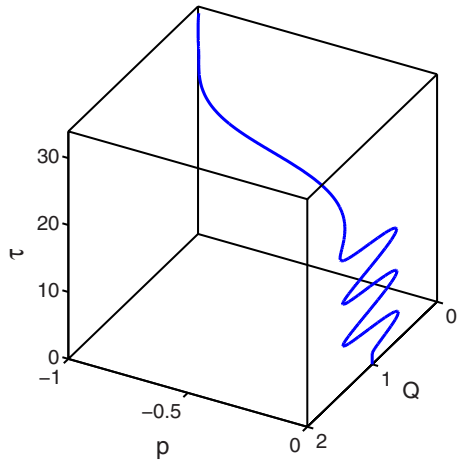

FIG. 6. (Color online) A nonperturbative instanton trajectory obtained by solving numerically the rescaled Hamilton equations (50) for $\varepsilon=0.6$ and $\alpha=1$. The trajectory first performs large-amplitude oscillations around the mean-field fixed point A of the unperturbed system [or, in other words, stays close to the perturbed fixed point of the Poincaré map $A_\varepsilon(t_0)$], then leaves the vicinity of the fixed point, and ultimately reaches (a close vicinity of) the fluctuational point $B(Q=0,p=-1)$ which, for the branching-annihilation reaction, remains unperturbed.

we computed the action numerically by solving the Hamilton equations. Rescaling time $\tau=\lambda_0 t$ and the coordinate $Q=\mu_0 q/\lambda_0=q/\Omega$ in Eqs. (14)–(16), one obtains rescaled Hamilton equations

$$\frac{\partial Q}{\partial \tau} = (1+2p)Q - (1+p)Q^2 + \varepsilon(1+2p)Q\cos\alpha\tau,$$

$$\frac{\partial p}{\partial \tau} = -(1+p)p + (2+p)pQ - \varepsilon(1+p)p\cos\alpha\tau, \quad (50)$$

which follow from the rescaled Hamiltonian

$$h(Q,p,\tau) = (p+1)pQ - \frac{1}{2}(2+p)pQ^2 + \varepsilon(p+1)pQ\cos\alpha\tau.$$

The action along the perturbed instanton $[Q_*(t),p_*(t)]$ is given by

$$\mathcal{S} = \Omega\int_{-\infty}^{\infty}\{-Q_*(\tau)\dot{p}_*(\tau) - h[Q_*(\tau),p_*(\tau),\tau]\}d\tau, \quad (51)$$

where the integrand is fully determined by two dimensionless parameters: the rescaled modulation amplitude ε and rescaled frequency $\alpha=\omega/\lambda$. The numerical solution is obtained by shooting. We start at $\tau=0$ at a point $[Q(0),p(0)]$ lying on a small circle of radius $\delta\ll 1$ centered in the unperturbed mean-field point $A(Q=1,p=0)$. The polar angle θ of the point $[Q(0),p(0)]$ on the circle serves as the only shooting parameter: it is varied until the numerical trajectory reaches, at some time $\tau=\tau_f$, (a close proximity of) the fluctuational point $B(Q=-1,p=0)$. For the numerically found instanton $[Q_*(t),p_*(t)]$ to be a good approximation to the true perturbed instanton in its entirety, δ must be sufficiently small. On the other hand, too a small δ causes a long τ_f (and therefore a long computation time and possible accumulation of numerical errors) because of the intrinsic logarithmic slowdown near the fixed point. By repeating the computations for a smaller circle, $\delta_1<\delta$, we checked that the same numerical instanton trajectory is reconstructed with high accuracy, apart from additional oscillations that appear in the vicinity of the mean-field point of the unperturbed system (see Figs. 6 and 7). As long as δ is chosen to be sufficiently small, the contribution of these oscillations to the net action along the instanton is small.

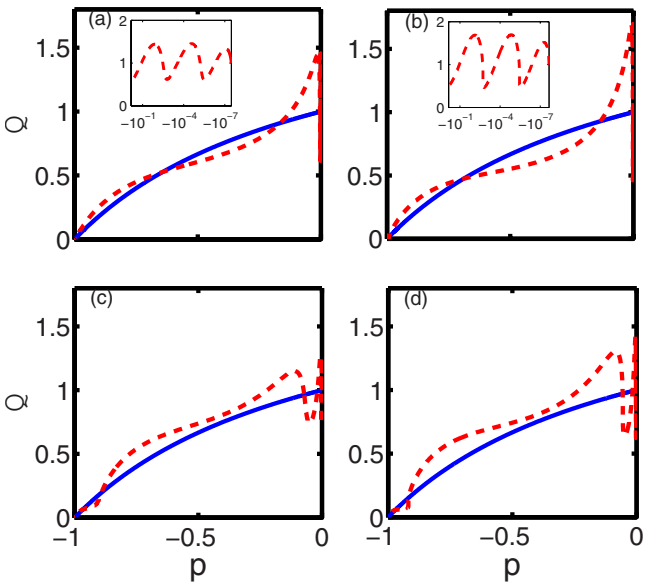

FIG. 7. (Color online) Projections on the (Q,p) plane of instantons found numerically for four sets of parameters (the dashed lines). The parameters and the corresponding rescaled actions [see Eq. (51)] $\mathcal{S}/\Omega$ are (a) $\varepsilon=0.6$, $\alpha=1$, $\mathcal{S}/\Omega=0.467$ (b) $\varepsilon=0.9$, $\alpha=1$, $\mathcal{S}/\Omega=0.398$ (c) $\varepsilon=0.6$, $\alpha=2$, $\mathcal{S}/\Omega=0.576$, and (d) $\varepsilon=0.9$, $\alpha=2$, $\mathcal{S}/\Omega=0.545$. The solid line denotes the unperturbed instanton (10). For comparison, the unperturbed rescaled action is $\mathcal{S}_0/\Omega=2(1-\ln 2)=0.6137\ldots$. The blowups in the vicinity of $p=0$ (the insets) show that $Q(p)$ oscillates before departing toward the fluctuational fixed point. In these examples $\delta=10^{-6}$.

We used this algorithm to verify our perturbative theoretical results; see Figs. 3–5. We also computed the perturbed instanton numerically in the parameter region beyond the validity of the perturbation techniques: $\varepsilon\lesssim 1$ and $\alpha\lesssim 1$. These computations strongly suggest that the instanton connection persists for any $\varepsilon<1$ and any α. Figures 6 and 7 show examples of numerically found instantons, and action along them, for nonperturbative values of parameters.

IV. ADIABATIC APPROXIMATION

Adiabatic approximation is nonperturbative in the modulation amplitude ε, and demands that the modulation frequency be much smaller than the characteristic relaxation rate of the system. Consider first a general single-species birth-death process with *time-independent* rates which possesses a nontrivial quasistationary state and a single absorb-

ing state at zero. At times much longer than the time of relaxation to the quasistationary state, the extinction probability at time t can be represented as

$$\mathcal{P}_0(t) = 1 - Ce^{-r_{ex}^{(0)}t},$$

where $r_{ex}^{(0)} = r_{ex}^{(0)}(\lambda_1, \lambda_2, \ldots)$ is the extinction rate: the lowest excited eigenvalue E_1, see, e.g., Refs. [15,21]. The extinction rate depends on the reaction rates of the problem $\lambda_1, \lambda_2, \ldots$. The constant C is determined by the initial conditions; for a sufficiently large initial number of particles, C is close to unity [15,21].

Now we introduce an adiabatically slow variation into the reaction rates so that the characteristic time of the variation is much longer than the relaxation time of the system, but much shorter than the MTE. The extinction probability can now be written as

$$\mathcal{P}_0(t) = 1 - Ce^{-\int_0^t r_{ex}(t')dt'}, \tag{52}$$

where $r_{ex}(t) = r_{ex}[\lambda_1(t), \lambda_2(t), \ldots]$ is the instantaneous value of the slowly time-dependent extinction rate. The average extinction rate $\bar{r}_{ex}$ can be defined via the relation

$$\mathcal{P}_0(t) = 1 - Ce^{-\bar{r}_{ex}t}. \tag{53}$$

Comparing Eqs. (52) and (53), we obtain

$$\bar{r}_{ex} = \frac{1}{T}\int_0^T r_{ex}(t')dt', \tag{54}$$

where T is much longer than the relaxation time but much shorter than the MTE. For slow periodic rate modulations with frequency ω Eq. (54) can be rewritten as

$$\bar{r}_{ex} = \frac{2\pi}{\omega}\int_0^{2\pi/\omega} r_{ex}(t')dt'. \tag{55}$$

The MTE is equal, in the adiabatic approximation, to $1/\bar{r}_{ex}$.

Now we illustrate the adiabatic approximation on our branching-annihilation example. Here the periodic solution of the mean-field equation (17) is $q(t) \simeq \Omega(1+\varepsilon\cos\omega t)$: the mean-field fixed point follows the slowly changing rate $\lambda(t)$ adiabatically.

The extinction rate of the branching-annihilation system with time-independent rates was found, including the preexponent, in Refs. [13–15]:

$$r_{ex}^{(0)} = \frac{\Omega^{3/2}}{2\sqrt{\pi}}e^{-\mathcal{S}_0}, \tag{56}$$

where $\mathcal{S}_0 = 2\Omega(1-\ln 2)$ and $\Omega = \lambda/\mu \gg 1$. We introduce a slow sinusoidal modulation in the branching rate λ, see Eq. (13), while keeping $\mu = \mu_0$ constant. The instantaneous extinction rate becomes

$$r_{ex}(t) = \frac{\Omega^{3/2}}{2\sqrt{\pi}}(1+\varepsilon\cos\omega t)^{3/2}e^{-\mathcal{S}_0(1+\varepsilon\cos\omega t)}. \tag{57}$$

For this result to be valid it is necessary that the argument in the exponent be large: $\mathcal{S}_0(1+\varepsilon\cos\omega t) \gg 1$, which yields

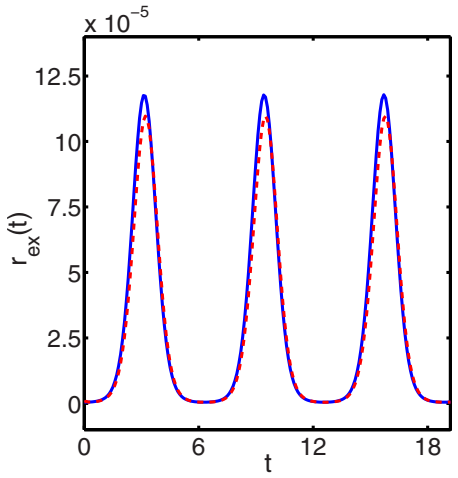

FIG. 8. (Color online) Comparison of the adiabatic instantaneous extinction rate, given by Eq. (57) (the solid line) and the instantaneous extinction rate determined from a numerical solution of the master equation Eq. (2). The numerical instantaneous extinction rate (the dashed line) was computed as $-(d/dt)\ln[1-\mathcal{P}_0(t)]$. The parameters are $\Omega = 25$, $\varepsilon = 0.2$, and $\alpha = 0.04$.

$$1 - |\varepsilon| \gg 1/\Omega. \tag{58}$$

The instantaneous extinction rate (57) can be also obtained, with exponential accuracy, in the following way. One treats the time in the time-dependent eikonal Hamiltonian (14) as a parameter and looks for zero-energy trajectories as in the time-independent case. In this way one obtains the "adiabatic instanton"

$$q = q_a(p;t) = \frac{2\Omega(1+p)}{(2+p)}(1+\varepsilon\cos\omega t), \tag{59}$$

and finds the adiabatic action $S_0(t) = -\int_0^{-1} q_a(p;t)dp = \mathcal{S}_0(1+\varepsilon\cos\omega t)$ which yields (the minus of) the logarithm of the instantaneous extinction rate, in agreement with Eq. (57). This simple derivation yields a necessary condition for the validity of the adiabatic approximation. Indeed, the adiabatic picture demands that ω be much less, at all times, than the adiabatically varying relaxation rate $\lambda(t) = \lambda_0(1+\varepsilon\cos\omega t)$. Therefore we must require $\omega \ll \lambda_0(1-|\varepsilon|)$, that is,

$$\alpha \ll 1 - |\varepsilon|. \tag{60}$$

For small or moderate modulation amplitudes, $|\varepsilon| \lesssim 1$, one recovers the same low-frequency criterion $\alpha \ll 1$ that led to Eq. (34). As $|\varepsilon|$ closely approaches 1, however, the criterion (60) becomes much more stringent. The criteria (58) and (60) can be rewritten as

$$1 - |\varepsilon| \gg \max(\Omega^{-1}, \alpha). \tag{61}$$

To verify Eq. (57), we solved numerically (a truncated version of) the original master equation (2). The numerical instantaneous extinction rate was computed from $-(d/dt)\ln[1-\mathcal{P}_0(t)]$. Figure 8 compares Eq. (57) with a numerical result for a small rescaled frequency $\alpha = 0.04$ and $\varepsilon = 0.2$, and good agreement is observed. The deviation in the

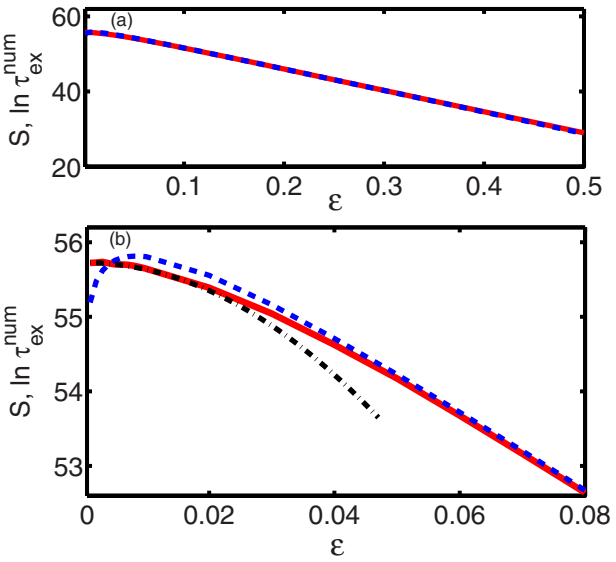

FIG. 9. (Color online) (a) Comparison between the action $\mathcal{S}$ given by Eq. (64) for $\varepsilon\Omega \gg 1$ (the dashed line) and the natural logarithm of the MTE found by solving the master equation numerically (the solid line), as a function of ε. (b) A blowup of the small-ε region: shown are the $\varepsilon\Omega \ll 1$ asymptote of the action $\mathcal{S}$ [Eq. (66)] (the dash-dotted line), the $\varepsilon\Omega \gg 1$ asymptote of the action $\mathcal{S}$ [Eq. (64)] (the dashed line), and the natural logarithm of the MTE found by solving the master equation numerically (the solid line), as a function of ε. The parameters in (a) and (b) are $\Omega=100$ and $\alpha=0.05$. One can see that Eq. (66) breaks down when $\varepsilon\Omega$ ceases to be small, whereas for $\varepsilon\Omega \gg 1$ the ε dependence becomes approximately linear, and the action is well described by Eq. (64).

peaks is mainly caused by $1/\Omega$ corrections to the eikonal theory: we checked that it goes down as Ω increases.

The average extinction rate (55) can be written as

$$\bar{r}_{ex} = \frac{\Omega^{3/2}}{4\pi^{3/2}} \int_0^{2\pi} (1 + \varepsilon \cos \tau)^{3/2} e^{-\mathcal{S}_0(1+\varepsilon \cos \tau)} d\tau. \quad (62)$$

This expression is ω-independent. For a comparison with the LT prediction (see below), it will be convenient to compute $-\ln(\bar{r}_{ex})$: the total action which includes, in addition to the leading-order contribution, a sub-leading contribution coming from the pre-exponent.

The integral in Eq. (62) can be calculated analytically in two limits. For $|\varepsilon|\Omega \gg 1$ one can employ the saddle point approximation and obtain

$$\bar{r}_{ex} = \frac{\Omega(1-|\varepsilon|)^{3/2}}{4\pi\sqrt{|\varepsilon|(1-\ln 2)}} e^{-\mathcal{S}_0(1-|\varepsilon|)}. \quad (63)$$

The saddle point is located at $t_* = \pm \pi/\omega$ (for $\varepsilon \gtrless 0$, respectively); the effective width of the Gaussian is $\sigma \sim (2|\varepsilon|\Omega\omega^2)^{-1/2} \ll \pi/\omega$. The resulting action is

$$\mathcal{S} = -\ln(\bar{r}_{ex}) = \mathcal{S}_0(1-|\varepsilon|) + \ln\left[\frac{\Omega(1-|\varepsilon|)^{3/2}}{4\pi\sqrt{|\varepsilon|(1-\ln 2)}}\right]. \quad (64)$$

The leading term $\mathcal{S}_0(1-|\varepsilon|)$ coincides with the zero-frequency limit predicted by the LT of Sec. III: see Eq. (34) with the α^2 term neglected. Its physical meaning is transparent: in view of the adiabatically slow rate modulation, the effective "activation barrier" to extinction $\mathcal{S}_0(1-|\varepsilon|)$ is determined by the minimal value of $\lambda(t)=\lambda_0(1+\varepsilon \cos \omega t)$ which is equal to $\lambda_0(1-|\varepsilon|)$. Equation (64), however, also includes an important pre-exponent (recall that $\Omega \gg 1$), missed by the leading order of the eikonal expansion. Note that, because of the additional pre-exponent, coming from the saddle-point integration, the Ω dependence of the resulting pre-exponent changes and becomes $\sim\Omega$ instead of $\sim\Omega^{3/2}$. Figure 9(a) compares the prediction of Eq. (64) with the natural logarithm of the MTE obtained by numerically solving the master equation, and excellent agreement is observed.

In the opposite limit, $|\varepsilon|\Omega \ll 1$, the integral (62) can be calculated via a Taylor expansion of the integrand in $\varepsilon\Omega$. Terms proportional to $\cos \tau$ vanish after the integration, and the leading-order result is

$$\bar{r}_{ex} \simeq r_{ex}^{(0)}[1 + \varepsilon^2\Omega^2(1-\ln 2)^2]. \quad (65)$$

This yields

$$\mathcal{S} = \mathcal{S}_0 - \varepsilon^2\Omega^2(1-\ln 2)^2. \quad (66)$$

Note that the strong inequality $|\varepsilon|\Omega \gg 1$ in Eq. (64) coincides with the validity criterion of the eikonal method in the linear theory (LT): the left inequality in Eq. (26). Correspondingly, when the opposite strong inequality $|\varepsilon|\Omega \ll 1$ holds, the correction to $\mathcal{S}_0$ that appears in Eq. (66) is much smaller than 1 and therefore strongly noneikonal. Figure 9(b) shows a comparison between Eq. (66) and the numerical solution of the master equation, and excellent agreement is observed.

One can notice that the leading-order term in the action (64), $\mathcal{S}_0(1-|\varepsilon|)$, goes down linearly in $|\varepsilon|$ for all $|\varepsilon|<1$. The linearity in $|\varepsilon|$ is nongeneric and stems from the fact that $\lambda(t)/\mu_0$ is linear in ε, and so is the exponent in the instantaneous extinction rate (62). In the general case, the $|\varepsilon|$ dependence of the exponent that appears in the instantaneous extinction rate is nonlinear, and therefore the linear $|\varepsilon|$ dependence of the action (which also appears in the LT regime of the eikonal approximation) will break down at $|\varepsilon| = \mathcal{O}(1)$. This is indeed what one observes if, instead of modulating λ, one modulates μ:

$$\lambda(t) = \lambda_0, \quad \mu(t) = \mu_0(1 + \varepsilon \cos \omega t). \quad (67)$$

In this case, using Eq. (55), we obtain the following action for $|\varepsilon|\Omega \gg 1$:

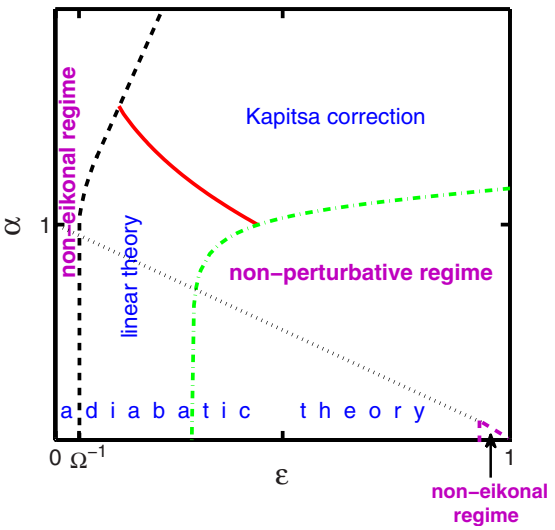

FIG. 10. (Color online) A schematic diagram of different regimes of extinction on the parameter plane $(\varepsilon>0,\alpha)$ of the branching-annihilation process. Either the LT or the Kapitsa method is applicable well to the left of and above the dash-dotted line (where the inequality $\Delta\mathcal{S}/\mathcal{S}_0\ll 1$ holds) and well to the right of the dashed line (where $\Delta\mathcal{S}\gg 1$). On the solid line $\varepsilon=f_1(\alpha)/f_2(\alpha)$, see Eqs. (47)–(49). The adiabatic approximation holds well below the dotted line. The horizontal size of the noneikonal regions at $\alpha\to 0$ is of order $1/\Omega$. The rest of the diagram is self-explanatory.

$$\mathcal{S}=-\ln(\bar{r}_{ex})=\frac{\mathcal{S}_0}{1+|\varepsilon|}+\ln\left[\frac{\Omega}{4\pi\sqrt{|\varepsilon|(1+|\varepsilon|)(1-\ln 2)}}\right]. \tag{68}$$

For $|\varepsilon|\ll 1$ the leading-order term $\mathcal{S}_0/(1+|\varepsilon|)\simeq\mathcal{S}_0(1-|\varepsilon|)$ coincides with the leading term of Eq. (64), or with Eq. (34) where one must put $\alpha=0$. For not small $|\varepsilon|$, however, the $|\varepsilon|$ dependence is nonlinear.

V. SUMMARY AND DISCUSSION

We have developed three complementary perturbation techniques for an analytical calculation of the exponential reduction in the mean time to extinction (MTE) in single-species birth-death processes (or reaction kinetics) that occur in a time-periodic environment. These are the linear theory (valid at small modulation amplitudes), the Kapitsa method (valid at high modulation frequencies), and the adiabatic approximation (valid at low modulation frequencies). We presented our theory on the example of a simple branching-annihilation process. Figure 10 shows different regimes of this process on the parameter plane $(\varepsilon>0,\alpha)$.

The linear theory and the Kapitsa method, as we used them, are rooted in the time-dependent eikonal theory that employs a large parameter Ω: the average number of individuals in the quasistationary state at times short compared with the MTE. The adiabatic approximation also employs the large parameter Ω. It yields, however, a more accurate result than the other two techniques as it yields a nontrivial Ω-dependent pre-exponent of the MTE. The higher accuracy, achieved in this way, is important in view of the fact that, at low frequencies, the reduction in the MTE is the largest.

An important result of this work is that, at high modulation frequencies and not too small modulation amplitudes, the linear theory can greatly underestimate the true reduction in the MTE. In this regime an accurate result is given by the Kapitsa correction, calculated in this work.

Our calculations of the modulation-induced reduction in the MTE are closely related to finding the optimal path to extinction, or instanton connection [9–11]. Although in generic Hamiltonians the existence of an instanton connection (a more standard mathematical term is a heteroclinic trajectory) can be guaranteed only at very small modulation amplitudes [19], our numerical results strongly indicate that, in the birth-death processes with an absorbing state at zero, a perturbed instanton persists at *any* reasonable modulation amplitude and at any frequency. This remarkable fact must be intimately related to the nongeneric structure of the birth-death Hamiltonians. More specifically, a future proof of the instanton persistence at arbitrary (physically reasonable) time-dependent perturbations of the reaction rates will most likely exploit the invariance of the zero-energy mean-field line $p=0$ and the zero-energy extinction line $q=0$ in the perturbed Hamiltonian.

ACKNOWLEDGMENTS

We are very grateful to Mark Dykman for enlightening discussions. M.A. was supported by the Clore Foundation. M.A. and B.M. were supported by the Israel Science Foundation (Grant No. 408/08); A.K. was supported by the NSF Grant No. DMR-0405212 and by the A. P. Sloan Foundation. M.A. and B.M. are grateful to the William I. Fine Theoretical Physics Institute of the University of Minnesota for hospitality.

[1] M. S. Bartlett, *Stochastic Population Models in Ecology and Epidemiology* (Wiley, New York, 1961).
[2] M. S. Samoilov and A. P. Arkin, Nat. Biotechnol. **24**, 1235 (2006); M. Assaf and B. Meerson, Phys. Rev. Lett. **100**, 058105 (2008).
[3] C. W. Gardiner, *Handbook of Stochastic Methods* (Springer Verlag, Berlin, 2004).
[4] N. G. van Kampen, *Stochastic Processes in Physics and Chemistry* (North-Holland, Amsterdam, 2001).
[5] *Population Viability Analysis*, edited by S. R. Beissinger and D. R. McCullough (University of Chicago Press, Chicago, 2002).
[6] E. G. Leigh, Jr., J. Toxicol. Environ. Health **90**, 213 (1981).
[7] R. Lande, Am. Nat. **142**, 911 (1993).
[8] K. Johst and C. Wissel, Theor Popul. Biol. **52**, 91 (1997); M. Schwager, K. Johst, and F. Jeltsch, Am. Nat. **167**, 879 (2006).

[9] C. Escudero and J. A. Rodríguez, Phys. Rev. E **77**, 011130 (2008).
[10] M. I. Dykman, E. Mori, J. Ross, and P. M. Hunt, J. Chem. Phys. **100**, 5735 (1994).
[11] V. Elgart and A. Kamenev, Phys. Rev. E **70**, 041106 (2004).
[12] I. Näsell, J. Theor. Biol. **211**, 11 (2001).
[13] J. W. Turner and M. Malek-Mansour, Physica A **93**, 517 (1978).
[14] D. A. Kessler and N. M. Shnerb, J. Stat. Phys. **127**, 861 (2007).
[15] M. Assaf and B. Meerson, Phys. Rev. E **75**, 031122 (2007).
[16] V. N. Smelyanskiy, M. I. Dykman, H. Rabitz, and B. E. Vugmeister, Phys. Rev. Lett. **79**, 3113 (1997).
[17] M. I. Dykman, B. Golding, L. I. McCann, V. N. Smelyanskiy, D. G. Luchinsky, R. Mannella, and P. V. E. McClintock, Chaos **11**, 587 (2001).
[18] V. Melnikov, Trans. Mosc. Math. Soc. **12**, 3 (1963).
[19] J. Guckenheimer and P. Holmes, *Nonlinear Oscillations, Dynamical Systems, and Bifurcations of Vector Fields* (Springer-Verlag, New York, 1986).
[20] L. D. Landau and E. M. Lifshitz, *Mechanics* (Pergamon, Oxford, 1976).
[21] M. Assaf and B. Meerson, Phys. Rev. E **74**, 041115 (2006); Phys. Rev. Lett. **97**, 200602 (2006).
[22] A. Kamenev and B. Meerson, Phys. Rev. E **77**, 061107 (2008).
[23] M. Dykman, I. B. Schwartz, and A. S. Landsman, Phys. Rev. Lett. **101**, 078101 (2008).
[24] M. Assaf, A. Kamenev, and B. Meerson, e-print arXiv:0803.0438.
[25] M. I. Dykman and M. A. Krivoglaz, Zh. Eksp. Teor. Fiz. **77**, 60 (1979) [Sov. Phys. JETP **50**, 30 (1979)].
[26] M. I. Freidlin and A. D. Wentzell, *Random Perturbations of Dynamical Systems* (Springer-Verlag, New York, 1984).
[27] R. Graham, in *Noise in Nonlinear Dynamical Systems*, edited by F. Moss and P. V. E. McClintock (Cambridge University Press, Cambridge, England, 1989), Vol. 1, p. 110.
[28] Invariance of the fluctuational fixed point under rate modulations is a nongeneric feature of the branching-annihilation model. In general (for instance, for the more general model $A \to 2A$, $2A \to 0$, and $A \to 0$ [24,29]) both the mean-field point and the fluctuational point are perturbed.
[29] V. Elgart and A. Kamenev, Phys. Rev. E **74**, 041101 (2006).
[30] Escudero and Rodríguez [9] showed, for a general (not necessarily sinusoidal) time-periodic modulation of the reaction rates $\lambda(t)$ and $\mu(t)$, that $M(t_0)$ is time periodic with zero mean. Therefore there exists some t_0^* for which $M(t_0^*)=0$.